

Brain, Behavior and Evolution



S. Karger
Medical and Scientific
Publishers
Basel • Freiburg
Paris • London
New York • New Delhi
Bangkok • Singapore
Tokyo • Sydney

KARGER

Intracellular Recording and Staining of Neurons in the Pigeon Nucleus lentiformis mesencephali

Zong-Xiang Tang Shu-Rong Wang

Laboratory for Visual Information Processing, Institute of Biophysics, Chinese Academy of Sciences, Beijing, P.R. China

Key Words

Brain slice · Intracellular recording · Nucleus lentiformis mesencephali · Optokinetic nystagmus · Pigeon · Vision

Abstract

The pretectal nucleus lentiformis mesencephali in pigeons is involved in optokinetic nystagmus and consists of lateral (nLMI) and medial (nLMm) subnuclei. The present study using intracellular recordings and brain slices shows that pretectal cells respond to depolarizing current injection in different ways. Type I cells (32%) fire spontaneously and have regular spikes. Type II cells (20%) discharge regular spikes, whose frequency increases as current intensity increases. Type III cells (8%) produce a series of bursts, each of which consists of 2–5 spikes depending on current intensities. Type IV cells (39%) fire several spikes in a cluster at the onset of current injection and are then rapidly adapted. One cell of type V (1%) shows spontaneous firing and is inactivated by depolarizing currents. Cells of types III and V are only found in nLMm, and other types of cells exist in both subnuclei. This physiological difference might be a bias due to the small sampling of cells. Twenty-six cells are labeled with dye and they could be categorized into fusiform (23.1%), piriform (7.7%), or multipolar (69.2%) cells. Some correlation seems to exist between the physiological and morphological properties of pretectal neurons. Statistically, the somatic size of nLMm cells is significant-

ly larger than that of nLMI cells, indicating that the nucleus could be divided cytoarchitecturally into magnocellular and parvocellular components as suggested previously.

Copyright © 2002 S. Karger AG, Basel

Introduction

The nucleus lentiformis mesencephali (nLM) is located in the pretectum in birds and is homologous to the nucleus of the optic tract in mammals [see review by McKenna and Wallman, 1985]. It is composed of two cellular components, a magnocellular component medially and a parvocellular component laterally [Kuhlenbeck, 1939], which were subsequently re-termed the nucleus lentiformis mesencephali pars medialis (nLMm) and the nucleus lentiformis mesencephali pars lateralis (nLMI), respectively, because it seems that both have a similar cytoarchitecture [Gamlin and Cohen, 1988a]. This nucleus receives input from the retina [Gamlin and Cohen, 1988a], the visual wulst [Karten et al., 1973], and the nucleus of the basal optic root (nBOR) [Brecha et al., 1980; Wylie et al., 1997], and projects to nBOR, the dorsolateral thalamus, the inferior olive and other neural structures [Gamlin and Cohen, 1988b; Wild, 1989; Wylie, 2001]. Its neurons are selective for the direction and velocity of motion [Fu et al., 1998a,b; Winterson and Brauth, 1985; Wylie and Frost, 1996; Wylie and Crowder,

KARGER

Fax +41 61 306 12 34
E-Mail karger@karger.ch
www.karger.com

© 2002 S. Karger AG, Basel
0006-8977/02/0601-0052\$18.50/0

Accessible online at:
www.karger.com/journals/bbe

Shu-Rong Wang, Laboratory for Visual Information Processing
Institute of Biophysics, Chinese Academy of Sciences
15 Datun Road, Beijing 100101 (P. R. China)
Tel. +86 10 6488 9858, Fax +86 10 6486 0713
E-Mail wangsr@sun5.ibp.ac.cn, srwang@hotmail.com

2000], working together with nBOR neurons in generating optokinetic nystagmus, which stabilizes images on the retina by compensatory movements of the eyes [Baldo and Britto, 1990; Nogueira and Britto, 1991; Gu et al., 2001; Wang et al., 2001]. To our knowledge, it has been shown that the only physiological difference between both subnuclei is their different velocity preferences, i.e., nLMm cells prefer lower velocities whereas nLMI cells prefer higher velocities [Winterson and Brauth, 1985].

Recently it has been shown that the firing patterns of tectal cells projecting to the chick nucleus rotundus are correlated with their morphological types [Luksch et al., 2001]. The pigeon nucleus rotundus contains several functional domains [Wang and Frost, 1992; Wang et al., 1993; Laverghetta and Shimizu, 1999], but only two types of firing activity may exist within the nucleus [Hu and Wang, 2001]. Although the avian nLM has been extensively studied anatomically [Karten et al., 1973; Wylie et al., 1997; Brecha et al., 1980; Gamlin and Cohen, 1988a,b; Wild, 1989; Wylie, 2001], physiologically [Winterson and Brauth, 1985; Baldo and Britto, 1990; Nogueira and Britto, 1991; Wylie and Frost, 1996; Fu et al., 1998a,b; Wylie and Crowder, 2000; Gu et al., 2001; Wang et al., 2001] and behaviorally [Gioanni et al., 1983], our knowledge of the firing behaviors and morphological features of nLM neurons is still lacking. The present study was undertaken by using intracellular recording and staining techniques on brain slices to reveal the firing patterns of the pigeon nLM cells in response to depolarizing current injection and ascertain whether the firing patterns are correlated with morphological features of nLM cells.

Materials and Methods

In the present study, 30 adult pigeons (*Columba livia*) were used following the policy on the use of animals in neuroscience research approved by the Society for Neuroscience. The experimental procedures were described previously [Hu et al., 2000; Hu and Wang, 2001]. Briefly, each pigeon was anesthetized with ketamine hydrochloride (40 mg/100 g body weight) and then decapitated. The brain was immediately removed from the skull, and washed in ice-cold Krebs-Ringer solution containing (in mM) NaCl, 124; KCl, 5; CaCl₂, 2; MgSO₄, 2; KH₂PO₄, 1.25; NaHCO₃, 26; glucose 10 [Hardy et al., 1987], oxygenated with a mixture of 95% O₂ and 5% CO₂. A block of the brain containing nLM was glued onto the stage of a Vibroslice (Campden Instruments Ltd., 752M, LE12 7IZ, UK). Slices were coronally sectioned at 400 μ m in thickness, and then transferred from a storage container to the recording chamber (BSC-HT, Medical System Corp., Greenvale, N.Y., USA) perfused with Krebs-Ringer solution bubbled with 95% O₂ and 5% CO₂ at a rate of 2 ml/min. The slices were incubated at 35 \pm 1 °C for 60 min before recording.

For intracellular recording and staining, a micropipette (0.5–1 μ m tip diameter) filled with either 3 M potassium acetate (impe-

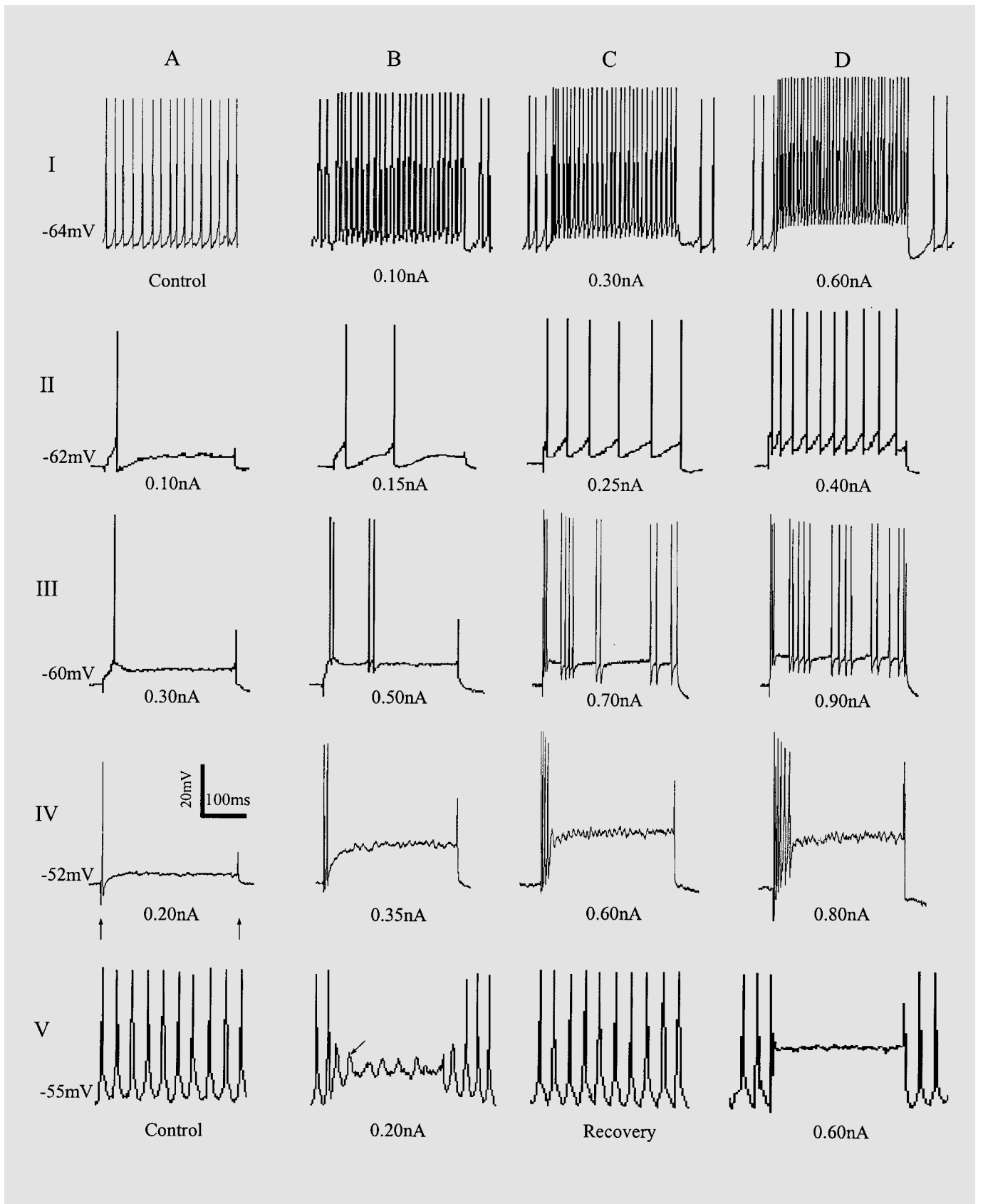
dance = 25–75 M Ω) or a solution of 3% Lucifer yellow (dilithium salt, Sigma Chemical Co., St. Louis, Mo., USA) plus 0.1 M LiCl (impedance = 95–250 M Ω) [Onn and Grace, 1994] was advanced into either nLMm or nLMI in slices. Both nuclei were readily discerned under the microscope, with nLMI appearing paler than nLMm. Neurons were impaled by applying brief positive current pulses (4 nA in intensity, 0.3 s in duration) and intracellular impalement was signaled by a sudden d.c. drop of 30–76 mV. The firing responses of nLM cells were examined by injecting depolarizing current pulses of 0.05–1.0 nA in several intensity steps and 200–400 ms in each injection duration. The current injection was applied by a stimulus signal delivering from a pulsemaster (WPI A300, Sarasota, Fla., USA) and stimulus isolator (WPI A360) to the stimulus input of an amplifier (WPI Intra electrometer 767). During current injection, the intracellular recordings were made in bridge mode because the electrodes had such a high impedance. Intracellular potentials or spikes were amplified with the amplifier, displayed on a digital oscilloscope (VC-7104, Hitachi Denshi Ltd., Tokyo) and stored on magnetic tapes (TEAC RD-135T Data Recorder, TEAC Corp., Tokyo), and then off-line analyzed with a computer.

In some experiments, the dye was injected by passing negative current pulses of 2–4 nA in intensity and at 1–2 Hz for 2–20 min, with one injection in one slice in most cases. After 0.5–2 h survival, the slices were removed from the recording chamber, fixed in 4% paraformaldehyde and kept in a refrigerator overnight. They were rinsed with physiological saline and then placed in 100% dimethylsulfoxide (DMSO) for 20 min [Grace and Llinàs, 1985]. The slices were coverslipped and dye-marked cells photographed at different depths of focus with a fluorescence microscope (Nikon Microphoto FXA, BV filter). The morphology of nLM cells was then scanned with a scanner (StudioStar, AGFA, Hong Kong) into a computer and reconstructed with the software tools of Adobe Photoshop 5.0.

Results

Ninety-one nLM cells were examined for their responses to depolarizing current injection, 26 of which were stained with Lucifer yellow to show their morphological features and distribution in the nucleus. Their recording depths ranged from 24 to 305 μ m with an average depth of 156 \pm 67 μ m (mean \pm SD, n = 91) to the surface, and the negative membrane potentials were averaged to be -54 ± 10 mV (n = 91) ranging from -30 to -76 mV.

These cells could be categorized into five types according to their responses to depolarizing current injection. Type I contained 29 spontaneous and regular-spiking cells (32%) including 6 cells in nLMI and 23 cells in nLMm. They fired spontaneously at an average rate of 40 \pm 24 Hz (spikes/s, n = 29) ranging from 13 to 100 Hz. Their firing rates were increased as current intensity increased. For example, the rates increased by 20–85 Hz over the spontaneous rate at currents of 0.05–0.15 nA, and by 48–152 Hz at 0.30–0.60 nA (fig. 1-I).



Type II included 18 regular-spiking cells (20%), with 3 cells being located in nLMI and 15 cells in nLMm. Lower current intensities (0.05–0.20 nA) induced a single spike at the onset of injection, and higher intensities (0.15–0.30 nA) could produce a series of spikes (6–38 Hz) with almost identical interspike intervals. Further increases in current intensity (0.40–1.00 nA) resulted in higher spike rates of 25–128 Hz (fig. 1-II).

Type III were 7 regular-bursting cells (8%) which were all located in nLMm. Lower current intensities (0.20–0.50 nA) induced a single spike at the onset of current injection, and higher intensities (0.50–0.70 nA) produced 2–5 bursts, each of which consisted of 2–4 spikes. Further increase in current intensities (0.70–1.00 nA) led to an increase both in the number of bursts (4–8 bursts) during depolarization and in the number of spikes in each burst (2–8 spikes) (fig. 1-III).

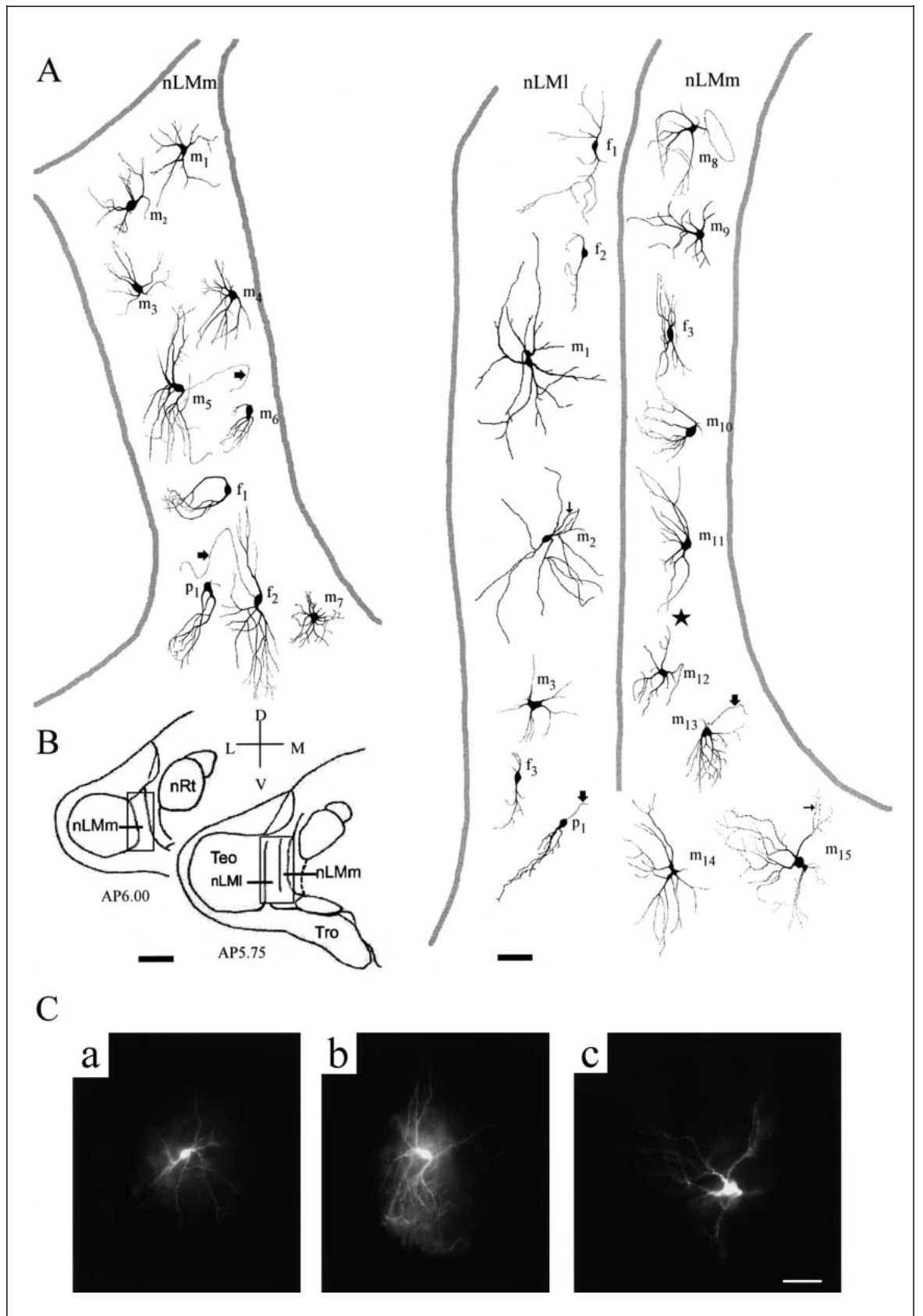
Thirty-six cells (39%) including 9 nLMI cells and 27 nLMm cells belonged to frequency-adaptation cells of type IV. In some of these cells, lower current intensities (0.10–0.20 nA) induced a single spike at the onset of depolarization. Higher intensities (0.30–0.50 nA) produced 2–3 spikes with frequencies of 64–87 Hz. Further increases in intensity (0.70–1.00 nA) evoked 4–5 spikes with frequencies of 89–213 Hz in a cluster at the beginning phase of current injection (fig. 1-IV). Other cells fired a single spike in response to currents ranging from 0.20 to 1.50 nA, and a cluster of spikes occurred during the administration of current at high intensities (1.20–2.50 nA).

Type V consisted of one firing-inactivation cell (1%) in nLMm. It spontaneously fired at rates of 30–33 Hz. During application of current at lower intensities (0.10–0.25 nA), spontaneous spikes were reduced in amplitude to hump-like depolarizations. These humps were further reduced by increasing current intensity and completely disappeared at about 0.6 nA. This inactivation could be released after current administration was stopped (fig. 1-V).

Fig. 1. Five firing patterns (I–V) of neurons in the pigeon nucleus lentiformis mesencephali in response to depolarizing current injection. I: Spontaneous and regular-spiking pattern. II: Regular-spiking pattern. III: Regular-bursting pattern. IV: Frequency-adaptation pattern. V: Bursting-inactivation pattern. Current intensities (nA) are shown in increasing magnitude (A–D) below each of recording traces. The resting potentials (mV) of these cells are indicated at the left to the first recording trace of each cell. Upward arrows point to electrical artifacts at the onset and the end of current injection. Oblique arrow points to a hump-like depolarization. Scales: 20 mV, 100 ms.

Twenty-six of the recorded cells were intracellularly stained with dye, including 7 nLMI cells and 19 nLMm cells. Morphologically, they could be generally categorized into fusiform, piriform, or multipolar cells according to the shape of cell bodies, and the number and distribution of primary dendrites (fig. 2). Fusiform cells (23.1%) were characterized by fusiform perikarya that issued a primary dendrite from each of the two poles (f_{1-3} in nLMm and f_{1-3} in nLMI). An axon was observed originating from the cell body sideways and traveling dorsolaterally in a zigzag way (f_2 in nLMm). Piriform cells (7.7%) possessed piriform perikarya that usually gave rise to an apical dendrite from the tapering pole and in some cases an axon from the other pole (p_1 in nLMm and p_1 in nLMI). The dendrites and their branches gathered in a column. Multipolar cells (69.2%) were characterized by round ($m_{2,4,9}$ in nLMm), spindle-shaped (m_2 in nLMI), pear-shaped ($m_{5,6,10}$ in nLMm), or polygonal ($m_{1,3,7,8,11-15}$ in nLMm and $m_{1,3}$ in nLMI) perikarya issuing more than two primary dendrites giving rise to secondary and tertiary dendrites. These dendrites and branches form circular (m_7 in nLMm) or elliptic (m_1 in nLMI) dendritic fields. In some of the cells an axon could be traced for a short distance. They traveled from the perikarya medially or laterally in a tortuous trajectory ($m_{5,13}$). The dendrites in a few multipolar cells bore some varicosities (m_{15} in nLMm and m_2 in nLMI). Average somatic diameter of nLMm cells was $24.4 \pm 3.2 \mu\text{m}$ ($n_1 = 19$) ranging from 17 to 29 μm , and that of nLMI cells was $18.3 \pm 3.8 \mu\text{m}$ ($n_2 = 7$) ranging from 15 to 26 μm . Unequal population tests showed that somatic size was significantly larger in nLMm than in nLMI ($t = 3.76$, $n_1 = 19$, $n_2 = 7$, $p < 0.01$). However, some multipolar cells in nLMI also had quite large dendritic fields ($m_{1,2}$), and their dendrites were thicker (m_1) and less frequently branched (m_2).

A degree of correlation seems to exist between the firing patterns and the morphological features of nLM cells examined. For example, cells $m_{1,4,5,7,9,12,15}$ and f_2 in nLMm and m_1 and p_1 in nLMI were all physiological type I cells that fired spontaneous, regular spikes in response to depolarizing current injection. They were predominantly multipolar cells. Multipolar cells $m_{2,3,10}$ in nLMm and m_2 in nLMI were physiologically classified as regular-spiking cells (type II). Cells of physiological type III responding with bursting patterns were characterized by diverse morphologies, including fusiform cell f_1 , piriform cell p_1 and multipolar cell m_{13} in nLMm. Among cells of physiological type IV were multipolar cells $m_{6,8,11,14}$ and fusiform cell f_3 in nLMm, and multipolar cell m_3 and fusiform cells f_{1-3} in nLMI. These multipolar and fusiform cells dis-



charged a group of spikes and then rapidly adapted in response to somatic current injection. Generally speaking, although there might be some correlation between the physiological and morphological properties of nLM cells, the present results also showed that morphologically diverse cells could fire spikes in a similar or identical mode, and nLM cells of similar morphology could respond in different ways to depolarizing current injection.

Discussion

The present study shows the existence of five different physiological types of nLM cells as defined by their firing patterns in response to depolarizing current injection. Visual cells in the pigeon nLM show considerable spontaneous activity [Winterson and Brauth, 1985; Fu et al., 1998a,b]. The present study indicates that one third of neurons recorded in brain slices fire spontaneously, demonstrating that spontaneous activity is an intrinsic property of nLM cells. This type of cell and type II cells all respond to depolarizing current injection in a tonic mode, i.e., their firing frequencies increase as current strength is increased. This firing mode is most frequently observed in neurons because it performs a linear summation of excitatory responses [Sherman, 2001]. The firing pattern of the regular-bursting cells is similar to chattering cells in the visual cortex [Gray and McCormick, 1996; Mancilla et al., 1998] and the avian tectum [Hardy et al., 1987; Luksch et al., 2001]. Bursting might provide better signal detection, probably signaling that something has changed in the environment [Sherman, 2001]. It may also mediate synchronous firing in a group of neurons [Gray and McCormick, 1996], as well as synaptic plasticity [Lisman,

1997; Harris et al., 2001]. The frequency-adaptation pattern has also been described in tectal cells [Hardy et al., 1987; Saito and Isa, 1999]. The firing-inactivation pattern is recorded in one nLMm cell and has never been reported elsewhere. It might be an exceptional case of the spike-inactivation pattern observed in rats [Saito and Isa, 1999] and pigeons [Hu and Wang, 2001]. Although cells of type III and V are not found in nLMI, it seems that nLMm and nLMI might not be different in their firing patterns. This apparent difference could be the result of a bias due to the small sampling of cells. The numbers of nLMI cells and nLMm cells examined are not comparable (17 nLMI cells vs. 74 nLMm cells), because nLMI cells are much more difficult to successfully impale than nLMm cells, probably due to smaller perikarya and/or the lower density of neurons within nLMI.

Pretecal cells labeled in both nLMm and nLMI could be categorized into fusiform, piriform and multipolar cells. Statistically, the somatic size of nLMm cells is significantly larger than that of nLMI cells, even though nLMI also possesses large-sized cells. This difference in perikaryal size is somewhat supported by the fact that smaller nLMI cells are much more difficult to impale. Another possible explanation for the difficulty with impalement might be that the density of cells in nLMI is lower than in nLMm. This is supported by the fact that nLMI looks paler than nLMm in brain slices. It appears that the present results support Kuhlenbeck's nomenclature [1939] that nLM consists of a magnocellular component medially and a parvocellular component laterally. Gamlin and Cohen [1988a] reported that nLMm contains small cells and large cells, and nLMI contains cells similar to nLMm. Based on this similar cytoarchitecture, they re-termed the nucleus lentiformis mesencephali pars medialis and the nucleus lentiformis mesencephali pars lateralis, respectively. However, those authors did not do a quantitative and statistical analysis, so that we could not compare their data with ours.

The present study shows that some correlation seems exist between the physiological and morphological properties of nLM neurons. The correlation between physiology and morphology of neurons has been clearly revealed in the visual cortex [Connors and Kriegstein, 1986; Connors and Gutnick, 1990] and the optic tectum [Luksch et al., 2001], but not in the suprachiasmatic nucleus [Pennartz et al., 1998] or the nucleus rotundus [Hu and Wang, 2001]. It is likely that some correlation reported here might be a transition from a strong correlation between the physiological and morphological properties of neurons [Connors and Kriegstein, 1986; Connors and Gut-

Fig. 2. Computer-aided drawings of 26 electrophysiologically identified neurons and their distribution in the nucleus lentiformis mesencephali pars medialis (nLMm) and in the nucleus lentiformis mesencephali pars lateralis (nLMI). These cells can be categorized into fusiform cells (f_{1-3} in nLMm and f_{1-3} in nLMI), piriform cells (p_1 in nLMm and p_1 in nLMI), and multipolar cells (m_{1-15} in nLMm and m_{1-3} in nLMI) (A). Areas framed by rectangles in B are correspondingly enlarged in A. Asterisk in A represents the location of the type V cell in fig. 1. The photomicrographs of cells m_2 in nLMI, m_5 and m_{15} in nLMm are shown with letters a, b, and c, respectively (C). Thick arrows point to axons, and thin arrows indicate varicosities. Other abbreviations: nRt, nucleus rotundus; Teo, optic tectum; Tro, optic tract. D, L, V, and M represent dorsal, lateral, ventral, and medial, respectively. AP, anterior-posterior levels of the pigeon's brain atlas [Karten and Hodos, 1967]. Scale bars: 100 μ m in A and C; 1 mm in B.

nick, 1990; Luksch et al., 2001] to a non-correlation between them [Pennartz et al., 1998; Hu and Wang, 2001]. Failure to reveal the morphological correlates, if any, to physiological types might be due to the small sample of neurons in some studies.

Acknowledgments

This work was supported by the National Natural Science Foundation of China and by the Chinese Academy of Sciences.

References

- Baldo, M.V., and L.R. Britto (1990) Accessory optic-pretectal interactions in the pigeon. *Braz. J. Med. Biol. Res.*, *23*: 1037–1040.
- Brecha, N., H.J. Karten, and S.P. Hunt (1980) Projections of the nucleus of the basal optic root in the pigeon: An autoradiographic and horseradish peroxidase study. *J. Comp. Neurol.*, *189*: 615–670.
- Connors, B.W., and M.J. Gutnick (1990) Intrinsic firing patterns of diverse neocortical neurons. *Trends Neurosci.*, *13*: 99–104.
- Connors, B.W., and A.R. Kriegstein (1986) Cellular physiology of the turtle visual cortex: distinctive properties of pyramidal and stellate neurons. *J. Neurosci.*, *6*: 164–177.
- Fu, Y.X., H.F. Gao, M.W. Guo, and S.R. Wang (1998a) Receptive field properties of visual neurons in the avian nucleus lentiformis mesencephali. *Exp. Brain Res.*, *118*: 279–285.
- Fu, Y.X., Q. Xiao, H.F. Gao, and S.R. Wang (1998b) Stimulus features eliciting visual responses from neurons in the nucleus lentiformis mesencephali in pigeons. *Vis. Neurosci.*, *15*: 1079–1087.
- Gamlin, P.D.R., and D.H. Cohen (1988a) Retinal projections to the pretectum in the pigeon (*Columba livia*). *J. Comp. Neurol.*, *269*: 1–17.
- Gamlin, P.D.R., and D.H. Cohen (1988b) Projections of the retinorecipient pretectal nuclei in the pigeon (*Columba livia*). *J. Comp. Neurol.*, *269*: 18–46.
- Gioanni, H., J. Rey, J. Villalobos, D. Richard, and A. Dalbera (1983) Optokinetic nystagmus in the pigeon (*Columba livia*). II. Role of the pretectal nucleus of the accessory optic system (AOS). *Exp. Brain Res.*, *50*: 237–247.
- Grace, A.A., and R. Llin(s) (1985) Dehydration-induced morphological artifacts in intracellularly stained neurons: circumvention using rapid DMSO clearing. *Neuroscience*, *16*: 461–475.
- Gray, C.M., and D.A. McCormick (1996) Chattering cells: superficial pyramidal neurons contributing to the generation of synchronous oscillations in the visual cortex. *Science*, *274*: 109–113.
- Gu, Y., Y. Wang, and S.R. Wang (2001) Directional modulation of visual responses of pretectal neurons by accessory optic neurons in pigeons. *Neuroscience*, *104*: 153–159.
- Hardy, O., E. Audinat, and D. Jassik-Gerschenfeld (1987) Electrophysiological properties of neurons recorded intracellularly in slices of the pigeon optic tectum. *Neuroscience*, *23*: 305–318.
- Harris, K.D., H. Hirase, X. Leinekugel, D.A. Henze, and G. Buzsaki (2001) Temporal interaction between single spikes and complex spike bursts in hippocampal pyramidal cells. *Neuron*, *32*: 141–149.
- Hu, J., W.C. Li, Q. Xiao, and S.R. Wang (2000) Electrical interactions between neurons in the pigeon isthmo-optic nucleus. *Brain Res. Bull.*, *51*: 159–163.
- Hu, J., and S.R. Wang (2001) Firing patterns and morphological features of neurons in the pigeon nucleus rotundus. *Brain Behav. Evol.*, *57*: 343–348.
- Karten, H.J., and W. Hodos (1967) A Stereotaxic Atlas of the Brain of the Pigeon (*Columba livia*). The Johns Hopkins Press, Baltimore, MD.
- Karten, H.J., W. Hodos, W.J. Nauta, and A.M. Revzin (1973) Neural connections of the 'visual wulst' of the avian telencephalon. Experimental studies in the pigeon (*Columba livia*) and owl (*Speotyto cunicularia*). *J. Comp. Neurol.*, *150*: 253–278.
- Kuhlenbeck, H. (1939) The development and structure of the pretectal cell masses in the chick. *J. Comp. Neurol.*, *71*: 361–387.
- Laverghetta, A.V., and T. Shimizu (1999) Visual discrimination in the pigeon (*Columba livia*): Effects of selective lesions of the nucleus rotundus. *NeuroReport*, *10*: 981–985.
- Lisman, J.E. (1997) Bursts as a unit of neural information: making unreliable synapses reliable. *Trends Neurosci.*, *20*: 38–43.
- Luksch, H., H.J. Karten, D. Kleinfeld, and R. Wessel (2001) Chattering and differential signal processing in identified motion-sensitive neurons of parallel visual pathways in the chick tectum. *J. Neurosci.*, *21*: 6440–6446.
- Mancilla, J.G., M. Fowler, and P.S. Ulinski (1998) Responses of regular spiking and fast spiking cells in turtle visual cortex to light flashes. *Vis. Neurosci.*, *15*: 979–993.
- McKenna, O.C., and J. Wallman (1985) Accessory optic system and pretectum of birds: Comparisons with those of other vertebrates. *Brain Behav. Evol.*, *26*: 91–116.
- Nogueira, M.I., and L.R. Britto (1991) Extraretinal modulation of accessory optic units in the pigeon. *Braz. J. Med. Biol. Res.*, *24*: 623–631.
- Onn, S.P., and A.A. Grace (1994) Dye-coupling between rat striatal neurons recorded in vivo: Compartmental organization and modulation by dopamine. *J. Neurophysiol.*, *71*: 1917–1934.
- Pennartz, C.M., M.T. De Jeu, A.M. Geurtsen, A.A. Sluiter, and M.L. Hermes (1998) Electrophysiological and morphological heterogeneity of neurons in slices of rat suprachiasmatic nucleus. *J. Physiol.*, *506*: 775–793.
- Saito, Y., and T. Isa (1999) Electrophysiological and morphological properties of neurons in the rat superior colliculus. I. Neurons in the intermediate layer. *J. Neurophysiol.*, *82*: 754–767.
- Sherman, S.M. (2001) Tonic and burst firing: dual modes of thalamocortical relay. *Trends Neurosci.*, *24*: 122–126.
- Wang, Y.C., and B.J. Frost (1992) 'Time to collision' is signaled by neurons in the nucleus rotundus of pigeon. *Nature*, *356*: 236–238.
- Wang, Y., Y. Gu, and S.R. Wang (2001) Directional responses of basal optic neurons are modulated by the nucleus lentiformis mesencephali in pigeons. *Neurosci. Lett.*, *311*: 33–36.
- Wang, Y.C., S.Y. Jiang, and B.J. Frost (1993) Visual processing in pigeon nucleus rotundus: Luminance, color, motion, and looming subdivisions. *Vis. Neurosci.*, *10*: 21–30.
- Wild, J.M. (1989) Pretectal and tectal projections to the homologue of the dorsal lateral geniculate nucleus in the pigeon: an anterograde and retrograde tracing study with cholera toxin conjugated to horseradish peroxidase. *Brain Res.*, *479*: 130–137.
- Winterson, B.J., and S.E. Brauth (1985) Direction-selective single units in the nucleus lentiformis mesencephali of the pigeon (*Columba livia*). *Exp. Brain Res.*, *60*: 215–226.
- Wylie, D.R. (2001) Projections from the nucleus of the basal optic root and nucleus lentiformis mesencephali to the inferior olive in pigeons. *J. Comp. Neurol.*, *429*: 502–513.
- Wylie, D.R., and N.A. Crowder (2000) Spatiotemporal properties of fast and slow neurons in the pretectal nucleus lentiformis mesencephali in pigeons. *J. Neurophysiol.*, *84*: 2529–2540.
- Wylie, D.R., and B.J. Frost (1996) The pigeon optokinetic system: Visual input in extraocular muscle coordinates. *Vis. Neurosci.*, *13*: 945–953.
- Wylie, D. R., B. Linkenhoker, and K. L. Lau (1997) Projections of the nucleus of the basal optic root in pigeons (*Columba livia*) revealed with biotinylated dextran amine. *J. Comp. Neurol.*, *384*: 517–536.